Article

Salinity Stress Mitigation Using Encapsulated Biofertilizers for Sustainable Agriculture

Nermin Adel Hussein El Semary [1,2,*], Mohamed Helmi Hadj Alouane [3,4,*] , Olfa Nasr [3,4], Munirah F. Aldayel [1] , Fatimah H. Alhaweti [1] and Faheem Ahmed [3]

[1] Department of Biological Sciences, College of Science, King Faisal University, P.O Box: 400, Al-Ahsa 31982, Saudi Arabia; maldayel@kfu.edu.sa (M.F.A.); falhweti@kfu.edu.sa (F.H.A.)

[2] Department of Botany and Microbiology, Faculty of Science, Helwan University, Cairo 11795, Egypt

[3] Department of Physics, College of Science, King Faisal University, P.O Box: 400, Al-Ahsa 31982, Saudi Arabia; onasr@kfu.edu.sa (O.N.); fahmed@kfu.edu.sa (F.A.)

[4] Micro-Optoelectronic and Nanostructures Laboratory, Faculty of Sciences, University of Monastir, Monastir 5019, Tunisia

[*] Correspondence: nelsemary@kfu.edu.sa (N.A.H.E.S.); malouane@kfu.edu.sa (M.H.H.A.); Tel.: +966-135897488 (N.A.H.E.S.)

check for updates

Abstract: The harmful effect of salinity stress on crops needs to be mitigated. Therefore, the application of microbial inoculum in combination with nanomaterials and methyl salicylate was investigated. Initially, different seeds were exposed to salinity levels treated with variable microbial treatments using different modes of applications. The microbial treatments included application of cyanobacterial strain *Cyanothece* sp. and the rhizobacterium *Enterobacter cloacae*, alone or in combination with one another, and a final treatment using combined microbial inoculum supplied with methyl salicylate. Later, different nanomaterials were used, namely, graphene, graphene oxide, and carbon nanotubes in combination with biofertilizers on the highest salinity level. The nanomaterial with microbial treatment and methyl salicylate were applied partly as a mixture in soil and partly as capsules. Results showed that salinity stress had a drastic inhibitory effect on growth parameters, especially at −5 MPa level. Nonetheless, the microbial treatments significantly alleviated the deleterious effect of salinity stress, especially when combined with methyl salicylate. When the nanomaterials were added to biofertilizers at highest salinity level, the inhibitory effect of salinity was mostly alleviated. Smart use of synergistic biofertilizers alongside the right nanomaterial, both encapsulated and in soil, would allow for mitigation and alleviation of inhibitory effect of salinity.

Keywords: Biofertilisers; blue green algae; capsule; carbon nanotubes (CNTs); cyanobacteria, *Cyanothece* sp.; graphene; graphene oxide (GO); methyl salicylate; nanomaterials; rhizobacteria and salinity stress

1. Introduction

One of the major challenges of cultivating arid and semi-arid soils is salinity. Salinity can affect all the developmental stages of plant growth. Seed germination is one of the most crucial stages and vulnerable to salinity [1]. Salinity can induce water stress in germinating seeds through decreasing water intake as a result of the osmotic effect. Thakur and Sharma [2] reported that the decrease in germination percentage may be due to induction of a state of dormancy in seeds under salinity stress. Salinity induced a significant increase in Na^+, Cl^-, and proline concentrations, while it reduced the accumulation of K^+ and Ca^{2+} in leaves of all the cultivars [3]. Munns [4] suggested that there are two phases of salinity stress; the first is quick and leads to growth reduction due to osmotic effect,

and the second phase is much slower, characterized by salt accumulation leading to salt toxicity in plants. With regard to biofertilizers, [5] reported their advantages in being beneficial in increasing plant growth and crop yield through increased nutrient availability and soil fertility. They also reduce pollution through cutting down on the use of chemical fertilizers. In addition, they protect plants against many pathogens [6].

Cyanobacteria (blue green algae) are one of the most important biofertilizers. They were first observed to naturally enhance the growth of rice paddies, where they synthesize and liberate plant growth regulators such as gibberellins that can exert a natural beneficial effect on salt-stressed rice plants [7]. They are oxygenic photosynthetic microorganisms that are also reported to produce and liberate 3-indol acetic acid [8]. Interestingly, Stirk et al. [9] reported the detection of auxin and cytokinin activities by three cyanobacterial strains. Indeed, it was later revealed that cyanobacteria produce many metabolites, which include the phytohormones IAAs (Indole Acetic Acid), cytokinin and gibberellin-like compounds), as well as iron-chelators (schizokinen, anachelin and synechobactins) [10]. Another important biofertilizer is the group of bacteria that colonize root regions, called rhizobacteria. In their review, Ahmed and Kibret [6] enumerated the effects of rhizobacteria, either directly, through increasing the bioavailability of nutrients such as phosphorus and essential minerals as well as phytohormone production, or indirectly through decreasing the inhibitory action of pathogens. Recently, Khan et al. [11] found that halotolerant rhizobacterial strains mitigated the salt stress on plants.

Methyl salicylate (MeSA) is a derivative of salicylic acid, which is a volatile organic compound that is associated with induced resistance plant defense methods (Abdul Malik et al. [12] and references therein). In addition, seed treatment with MeSA can be used to enhance rice seed germination and seedling growth [13].

Kalaivani et al. [13] suggested that external application of methyl salicylate is responsible for increased SA (Salicylic acid) which acts as a potential antioxidant and is associated with pathways that regulate and enhance many physiological processes in plants, including germination rate, cell growth, and mineral uptake [14].

In recent years, due to their excellent characteristics, carbon nanostructures, including graphene, graphene oxide (GO), and carbon nanotubes (CNTs), have attracted enormous attention and been applied to a wide variety of fields [15–18]. These carbon nanostructures have been successfully used as a filler for the reinforcements in polymer matrices due to their outstanding thermal and mechanical properties, high specific surface areas, chemical stability, and superior electrical conductivity [19–21]. Due to these properties, graphene (a single atomic layer of graphite with an ideal 2D sp2-hybridized structure) and CNTs (cylindrical graphene tubes with a 1D sp2-hybridized structure) have been marked as potential candidates for various applications, such as electronics, sensors, energy storage and conversion devices, and biological applications [22]. Graphene oxide (GO, an oxidized single-layered or multilayered graphene) and reduced graphene oxide (rGO) are practically the most studied graphene derivatives. Carbon nanostructures possess an exceptional photothermal response and show great biomedical applications, including in biosensors for proteins, aptamers, nucleic acid, antibodies, and biomarkers [23]. Various reports are available on the successful utilization of these carbon nanostructures, including biomolecular analysis, discovery of biomarkers, bioimaging, biological carriers, tissue engineering, target delivery, and photothermal therapy [24,25]. Given their functionalization with biological systems, the present research would investigate the novel combined application of nanomaterials and biofertilisers for the purpose of mitigating salinity.

2. Materials and Methods

2.1. Culture of Cyanobacterial Strain (Blue Green Algal Strain)

A monospecific culture of *Cyanothece* sp. that was previously isolated [26] was used in the current study. The cells were solitary with no colony formation. Ten mL of mid-logarithmic culture per pot was used in the experiments, either solely or in combination with rhizobacteria and methyl salicylate.

2.2. Culture of Rhizobacterium

Enterobacter cloacae is routinely grown in Luria Bertani (LB) medium (Fisher Scientific, Hampton, NH, USA) at 30 °C in a shaking incubator at 250 rpm.

2.3. Germination Experiments

The initial experiment was carried out using seeds of different families, including barley (*Hordeum vulgare*), Poaceae, monocot, and broad beans (*Vicia faba*, fabaceae, dicot.), which were germinated under different osmotic stress values (0.0, −0.1, −0.3, −0.5 MPa) to determine their salinity susceptibility. These seeds were exposed to three modes of applications of biofertilizers for a one-week course. The modes were as follows:

(a) Adding biofertilizers to soil and irrigating with saline water,
(b) Presoaking in biofertilizers for one day, then irrigating with saline water,
(c) Presoaking in biofertilizers for 12 h, then irrigating with saline water.

In all experiments, the seeds were sterilized with 5% Clorox, rinsed thoroughly, and the sand was washed and sterilized in oven. All modes of biofertilizer applications were exposed to the tested salinity levels. The biofertilizer treatments were as follows: no biofertilizers; with alga (cyanobacterium) alone; with rhizobacterium alone; with rhizobacterium and alga; with rhizbacterium, alga and MeSA. Methyl salicylate was supplied at 10 mg/L. Biofertilizers were mixed with soil prior to irrigation with water of different salinities.

The soil mode of application of biofertilizers was selected for further experiments, based on results, and the biofertilizer treatment formulated by the combination of rhizobacterium, alga, and methyl salicylate was used in subsequent experiments.

To test the effect of adding different nanomaterials to the biofertilizers under highest salinity stress, nanomaterials of three different types, namely, graphene, graphene oxide, and carbon nanotubes, were supplied in different concentrations. The detailed description of these materials is supplied in the coming section.

They were added as 2 mL of nanomaterial + 10 mL cyanobacterial (algal culture) + 10 mL rhizobacterial strain + 10 mL MeSA. The detailed compositions of the different mixtures were as follows with the concentrations of the nanomaterials mentioned.

- Graphene + alga + bacterium + MeSA (sample denoted 0.4 Gr-Al-B and 0.8 Gr-Al-B),
- CNT + alga + bacterium + MeSA (sample denoted 0.4 CNT-Al-B and 0.8 CNT-Al-B),
- GO + alga+ bacterium + MeSA (sample denoted 1 GO-Al-B and 2 GO-Al-B).

The different mixtures' optical properties were measured and those concentrations of nanomaterial that did not cause significant detrimental effect on algal (cyanobacterial) spectral bioactivity were used in further tests.

Those concentrations were mixed with biofertilizers supplemented with MeSA and were applied directly to the soil, where most of the combined components (90% of the total volume) were mixed thoroughly with soil, whereas the rest (10%) was used in the encapsulated form using agar 6% (*w/v*). Their effect was tested at the highest salinity level −5 MPa.

2.4. Preparation of Carbon Materials

2.4.1. Preparation of Graphene Oxide

Using the Hummers and Offeman's method, the graphite was oxidized to synthesize the GO. At first, 3.5 g of graphite was added to 100 mL of 98% H_2SO_4 with vigorous stirring. While maintaining a temperature below 20 °C, 10 g of $KMNO_4$ was added. After stirring for 2 h at 35 °C, the mixture was transferred to 500 mL of deionized water, and 20 mL of 30% H_2SO_4 was added to remove any excess permanganate. Upon treatment with the peroxide, the suspension turned bright yellow. The GO was then purified by filtration via a sintered glass filter. HCl was used to wash the filtrate, which was then washed with hot water to remove the residual sulfate ions, yielding a yellowish-brown filter cake. Finally, the resultant GO preparation was dried at 80 °C after repeated washings with hot water. The graphene (samples 0.4 Gr and 0.8 Gr) and CNT (samples 0.4 CNT and 0.8 CNT) concentrations used in this experiment were 0.4 and 0.8 mg/mL. For GO, 1 and 2 mg/mL were used (samples 1 GO and 2 GO). However, double the higher concentration of each nanomaterial was also used only in optical tests to check the extent to which there would be a change in spectral properties if much higher concentration was used.

2.4.2. Preparation of Carbon Nanotubes

Carbon nanotubes used in this experiments were MWCNTs (>95%, OD: 30–50 nm) purchased from US Research Nanomaterials, Houston, TX, USA. The MWCNTs had an outside diameter ranging from 30–50 nm, an inside diameter ranging from 5–12 nm, and a length of about 10–20 um. The specific surface area (SSA) of the MWCNTs was >60 m^2/g.

2.4.3. Preparation of Graphene

Graphene used in these experiments was graphene nanoflakes (99.9%) purchased from Graphene Supermarket, Ronkonkoma, NY, USA. Graphene nanoflakes had an average flake thickness of about ~8 nm (20–30 monolayers) and an average particle (lateral) size of about ~5 μm. The specific surface area (SSA) of graphene nanopowder was >15 m^2/g.

2.5. Spectroscopy Techniques

Raman spectra were recorded with a confocal Raman microscope at room temperature by using the HORIBA Jobin Yvon LabRAM HR equipped with a Syncerity Scientific CCD Deep Cooled Camera and an automated XY motorized stage. The lines of 633 and 785 nm laser were used as the source of excitation. Before the measurements were performed, the micro-Raman spectrometer was well calibrated using a 521 cm^{-1} Raman line of single crystalline Silicon (Si) wafer.

The UV-vis absorption spectra were measured using a Shimadzu UV-1800 spectrophotometer (200–800 nm) with 10 mm quartz cuvettes against demineralized water.

2.6. Statistical Analysis

Morphometric measurements were recorded for replicates, followed by statistical analysis. Data were checked for normality and analyzed for their significance using two-way ANOVA supplied in the statistical package Minitab 13.

3. Results

3.1. Germination Experiments

With regard to the first mode of application through irrigation, it was noticed that the combined microbial treatment of bacterial and cyanobacteria strains with MeSA resulted in the highest growth parameters under all levels of salinity except for dry weight in most of the treatments, both in barley and broad beans. Salinity stress had also a highly significant drastic impact on the morphometric

parameters. However, the application of the different levels of microbial treatments had significant positive impact on all parameters measured, and the microbial treatments, with either algal strain alone or rhizobacterium alone, did improve all parameters measured (Table 1). Barley was noticeably less affected by salinity than was broad beans.

With regard to the presoaking treatment for 12 h, there was an inhibition of germination in most of the treatments, with only the combined microbial treatment and MeSA giving noticeable growth at 0 and −0.1 MPa. However, at −3 and −5 MPa there was no germination in both barley and broad beans (Table 2). The effect of salinity stress was highly significant in inducing drastic changes in growth parameters. The microbial treatment did not induce much improvement, especially at higher salinity levels. The fresh and dry weights did not have any consistent pattern.

The last experiment was conducted to investigate germination at the highest salinity level, −5 MPa. This experiment was conducted using the combination of biofertilizers, MeSA, and nanomaterials. As the optical properties for every concentration of nanomaterial were tested (as discussed in detail in the following section), only those concentrations of nanomaterials that did not drastically affect the algal photosynthetic activity were used.

Table 1. Morphometric measurements of seedlings of barley and broad beans by adding them directly to soil. Standard deviation between brackets.

Type of Seed	Salinity Treatment MPa	Biofertilizer Treatment	Radicle Length (cm)	Plumule Length (cm)	Fresh Weight (g)	Dry Weight (g)	Germination%
Barley	0	0	0.69 (0.09)	1.59 (0.09)	0.09 (0.02)	0.02 (0.01)	50%
		Alga	10.05 (3.34)	14.64 (4.10)	0.21 (0.10)	0.033 (0.01)	90%
		Bacterium	9.77 (2.1)	15.55 (3.8)	0.17 (0.07)	0.032 (0.00)	100%
		Bacterium + Alga	9.30 (3.1)	18.48 (3.04)	0.23 (0.05)	0.032 (0.01)	100%
		Bacterium + Alga + MeSA	12.12 (3.6)	14.84 (2.43)	0.19 (0.02)	0.0260 0.00)	100%
	−1	0	0.65 (0.09)	0.52 (0.09)	0.08 (0.01)	0.037 (0.00)	70%
		Alga	1.14 (1.5)	0.54 (0.04)	0.09 (0.03)	0.034 (0.00)	80%
		Bacterium	2.0 (0.49)	1.95 (1.09)	0.09 (0.01)	0.031 (0.00)	60%
		Bacterium + Alga	2.35 (1.05)	2.19 (0.9)	0.10 (0.03)	0.031 (0.00)	70%
		Bacterium + Alga + MeSA	3.45 (1.3)	4.7 (1.7)	0.12 (0.05)	0.024 (0.00)	100%
	−3	0	1.02 (0.5)	0.15 (0.06)	0.09 (0.03)	0.034 (0.01)	90%
		Algae	1.22 (0.3)	0.14 (0.02)	0.09 (0.03)	0.037 (0.01)	70%
		Bacteria	1.0 (0.8)	0.04 (0.05)	0.078 (0.06)	0.038 (0.01)	60%
		Bacterium + Alga	3.62 (1.85)	0.21 (0.01)	0.089 (0.05)	0.037 (0.00)	90%
		Bacterium + Alga + MeSA	5.12 (0.88)	1.15 (0.43)	0.08 (0.00)	0.36 (0.03)	80%
	−5	0	0.2 (0.03)	0 (0)	0.065 (0.02)	0.039 (0.00)	60%
		Alga	1.0 (0.09)	0. 8 (0.03)	0.079 (0.03)	0.0331 (0.01)	70%
		Bacterium	0.43 (0.3)	0.4 (0.00)	0.081 (0.03)	0.036 (0.00)	60%
		Bacterium + Alga	0.29 (0.17)	0.4 (0.00)	0.078 (0.03)	0.04 (0.01)	60%
		Bacterium + Alga + MeSA	0.28 (0.20)	0.6 (0.01)	0.064 (0.01)	0.03 (0.00)	70%

Table 1. *Cont.*

Type of Seed	Salinity Treatment MPa	Biofertilizer Treatment	Radicle Length (cm)	Plumule Length (cm)	Fresh Weight (g)	Dry Weight (g)	Germination%
Broad beans	0	0	3.45 (1.3)	2.57 (1.3)	2.425 (0.9)	1.10 (0.04)	80%
		Alga	6.95 (3.3)	7.22 (1.1)	3.85 (0.05)	0.77 (0.38)	90%
		Bacterium	4.90 (1.1)	4.98 (1.3)	3.85 (0.05)	0.73 (0.38)	100%
		Bacterium + Alga	5.62 (0.78)	7.67 (1.08)	3.1 (1.4)	0.72 (0.17)	100%
		Bacteria + Algae + MeSA	7.95 (1.20)	8.59 (3.4)	3.8 (1. 6)	0.70 (0.2)	90%
	−1	0	0.33 (0.06)	0 (0)	1.84 (0.64)	0.98 (0.14)	50%
		Alga	0.28 (0.08)	0.13 (0.04)	1.75 (0.64)	0.73 (0.15)	40%
		Bacterium	0.55 (0.07)	0.24 (0. 04)	1.73 (0.18)	0.75 (0.10)	50%
		Bacterium + Alga	0.21 (0.02)	0.24 (0.05)	1.74 (0.9)	0.75 (0.23)	60%
		Bacterium + Alga + MeSA	1.93 (0.84)	1.37 (0.92)	1.88 (0.24)	0.74 (0.04)	40%
	−3	0	0.05 (0.01)	0 (0)	1.5 (0.33)	0.87 (0.20)	10%
		Alga	0 (0)	0 (0)	1.6 (0.30)	0.78 (0.17)	0
		Bacterium	0 (0)	0 (0)	1.56 (0.04)	0.75 (0.07)	0
		Bacterium + Alga	0.26 (0.78)	0 (0)	1.52 (0.60)	0.71 (0.20)	0
		Bacterium + Alga + MeSA	0.26 (0.08)	0 (0)	1.4 (0.20)	0.72 (0.03)	20%
	−5	0	0 (0)	0 (0)	1.41 (0.3)	0.85 (0)	0
		Alga	0 (0)	0 (0)	1.59 (0.14)	0.78 (0.14)	0
		Bacterium	0 (0)	0 (0)	1.60 (0.14)	0.77 (0.14)	0
		Bacterium + Alga	0 (0)	0 (0)	1.45 (0.19)	0.80 (0.18)	0
		Bacterium + Alga + MeSA	0 (0)	0 (0)	1.45 (0.03)	0.74 (0.06)	0

The germination of both plants in graphene and carbon nanotubes, combined with biofertilizer treatment under the highest salinity stress level, almost completely alleviated the salinity stress in comparison to growth with biofertilizers alone at −5 MPa in Table 2. In the case of barley, however, all treatments with different nanomaterials resulted in the germination and growth of seedlings despite the osmotic stress and the cumulative stress resulting from water and re-watering with concentrated saline.

Nevertheless, graphene oxide was the nanomaterial that enhanced germination and growth of barley most significantly (Table 3) in comparison with other nanomaterials. In the case of graphene at high concentration, it increased radicle length in both barley and broad beans. In all nanomaterial treatments, barley plumule length was significantly enhanced, as well as significant enhancement in its radicle length with graphene and moderate enhancement with graphene oxide. In case of broad beans, however, only graphene and CNT enhanced germination and radicle growth.

Table 2. Morphometric measurements of seedlings of barley and broad beans, using soaking for 12 h in biofertilizer as mode of application of biofertilizers. Standard deviation is found between brackets.

Type of Seed	Salinity Treatment MPa	Biofertilizer Treatment	Radicle Length (cm)	Plumule Length (cm)	Fresh Weight (g)	Dry Weight (g)	Germination %
Barley	0	0	0 (0)	0 (0)	0.22 (0.0)	0.042 (0.0)	0%
		Alga	1.02 (0.17)	2.02 (0.5)	0.64 (0.1)	0.06 (0.0)	20%
		Bacterium	0.06 (0. 03)	0.1 (0.07)	0.07 (0.03)	0.05 (0.02)	20%
		Bacterium + Alga	0 (0)	0 (0)	0.077 (0.03)	0.058 (0.04)	0%
		Bacterium + Alga + MeSA	2.43 (1.2)	3.33 (1.7)	0.075 (0.01)	0.049 (0.01)	20%
	−1	0	0 (0)	0 (0)	0.058 (0.02)	0.041 (0.007)	0%
		Alga	0 (0)	0 (0)	0.065 (0.03)	0.041 (0.01)	0%
		Bacterium	0 (0)	0 (0)	0.082 (0.012)	0.045 (0.018)	0%
		Bacterium + Alga	0.05 (0.01)	0 (0)	0.067 (0.007)	0.039 (0.007)	10%
		Bacterium + Alga + MeSA	0.1 (0.03)	0.09 (0.01)	0.074 (0.03)	0.044 (0.01)	30%
	−3	0	0 (0)	0 (0)	0.053 (0.007)	0.041 (0.007)	0%
		Alga	0 (0)	0 (0)	0.065 (0.007)	0.044 (0.028)	0%
		Bacterium	0 (0)	0 (0)	0.070 (0.01)	0.049 (0.01)	0%
		Bacterium + Alga	0 (0)	0 (0)	0.066 (0.03)	0.045 (0.003)	0%
		Bacterium + Alga + MeSA	0 (0)	0 (0)	0.07 (0.01)	0.04 (0.01)	0%
	−5	0	0 (0)	0 (0)	0.063 (0.01)	0.045 (0.00)	0%
		Alga	0 (0)	0 (0)	0.065 (0.00)	0.046 (0.00)	0%
		Bacterium	0 (0)	0 (0)	0.0612 (0.007)	0.042 (0.01)	0%
		Bacterium + Alga	0 (0)	0 (0)	0.064 (0.02)	0.05 (0.04)	0%
		Bacterium + Alga + MeSA	0 (0)	0 (0)	0.06 (0.01)	0.045 (0.01)	0%
Broad beans	0	0	0.69 (0.09)	0.53 (0.05)	1.95 (0.7)	0.652 (0.2)	80%
		Alga	1.29 (0.07)	1.34 (0.04)	1.72 (0.04)	0.70 (0.04)	100%
		Bacterium	0.82 (0.08)	0.91 (0.08)	1.88 (0.06)	0.777 (0. 05)	100%
		Bacterium + Alga	1.56 (0.94)	1.39 (0.50)	1.83 (0.3)	0.74 (0.2)	100%
		Bacterium + Alga + MeSA	1.58 (0.08)	1.32 (0.4)	1.73 (0.6)	0.73 (0.09)	90%
	−1	0	0.23 (0.02)	0(0)	1.631 (0.8)	0.6453 (0.08)	60%
		Alga	0.46 (0.05)	0.20 (0.06)	1.65 (0.2)	0.76 (0.1)	70%
		Bacterium	0.42 (0.18)	0 (0)	1.60 (0.4)	0.66 (0.2)	80%
		Bacterium + Alga	0.48 (0.15)	0.15 (0.02)	1.501 (0.01)	0.63 (0.15)	70%
		Bacterium + Alga + MeSA	0.52 (0.15)	0 (0)	1.5 (0.9)	0.70 (0.3)	80%

Table 2. *Cont.*

Type of Seed	Salinity Treatment MPa	Biofertilizer Treatment	Radicle Length (cm)	Plumule Length (cm)	Fresh Weight (g)	Dry Weight (g)	Germination %
Broad beans	−3	0	0 (0)	0 (0)	1.43 (0.9)	0.68 (0.09)	0
		Alga	0 (0)	0 (0)	1.536 (0.0)	0.784 (0.2)	0
		Bacterium	0 (0)	0 (0)	1.6 (0.0)	0.95 (0.1)	0
		Bacterium + Alga	0 (0)	0 (0)	1.39 (0.24)	0.94 (0.3)	0
		Bacterium + Alga +MeSA	0 (0)	0 (0)	1.559 (0.2)	0.99 (0.19)	0
	−5	0	0 (0)	0 (0)	1.41 (0.03)	0.67 (0.03)	0
		Alga	0 (0)	0 (0)	1.36 (0.6)	1.1 (0.5)	0
		Bacterium	0 (0)	0 (0)	1.39 (0.06)	1.10 (0.02)	0
		Bacterium + Alga	0 (0)	0 (0)	1.32 (0.43)	1.04 (0.36)	0
		Bacterium + Alga + MeSA	0 (0)	0 (0)	1.22 (0.04)	0.975 (0.02)	0

Table 3. The combination of nanomaterials and biofertilizers and its application as capsules to counteract salinity stress at the highest level of −5 MPa. GO (graphene oxide), Gr (graphene), and CNT (carbon nanotubes).

Salinity Treatment MPa	Type of Seed	Treatment [Nanomaterial (Concentration mg/mL)/Biofertilizer Treatment]	Radicle Length (cm)	Plumule Length (cm)	Fresh Wt. (g)	Dry Wt. (g)	Germination %
−5	Barley	GO (1) [Bacterium + Alga + MeSA]	4.8	4.2	0.094	0.047	60%
		GO (2) [Bacterium + Alga + MeSA]	5.8	3.0	0.096	0.047	70%
		CNT (0.8) [Bacterium + Alga + MeSA]	1.2	2.0	0.085	0.048	40%
		GR (0.8) [Bacterium + Alga + MeSA]	0.88	0.76	0.092	0.040	70%
	Broad beans	GO (1) [Bacterium + Alga + MeSA]	0	0	1.546	1.136	0%
		GO (2) [Bacterium + Alga + MeSA]	0	0	1.724	1.400	0%
		CNT (0.8) [Bacterium + Alga + MeSA]	1.0	0	1.630	1.226	10%
		GR (0.8) [Bacterium + Alga + MeSA]	1.8	0	1.529	1.144	20%

3.2. Optical Properties

Algal strain is considered as a biofertilizer with many spectral properties due to the presence of several pigments and its photosynthetic nature, and therefore the effect of including it with nanomaterial of certain optical properties must be monitored. Figure 1 shows the transmittance spectra of reference algal cells alone and with other components in the presence of different carbon nanomaterials as a function of wavelength. The transmittance of the algal cells alone was found to be 50%. This optical transmittance of algae was decreased by the graphene concentration of 0.4 to 0.8 mg/mL, but if bacterial cells were added, the optical transmittance of graphene at 8 mg/mL increased to the near normal algal transmittance. Also, optical transmittance of GO and CNT increased when the concentrations increased from 1 to 2 mg/mL and 0.4 to 0.8 mg/mL, respectively, especially in the presence of bacteria. GO, specifically, gave better transmission than the rest of the carbon nanomaterials. It is interesting to note that the maximum peaks associated with chlorophyll (a) in the visible region (600–700 nm) were clearly observed for a high concentration of GO mixed with the alga (2 GO-Al). It is important to report that GO is more hydrophilic than graphene and CNT due to the high level of oxygen-containing functional groups on the basal plane and is reported not to inflict damage on alga [27]. GO bears negative surface charges containing hydroxyl and epoxide functional groups and has a colloidal stability in biological media [28,29]. The transmittance spectra of the mixture of algal cells, nano-carbon material, and rhizobacterium were studied (Figure 1). The transmittance properties were clearly improved by introducing rhizobacterium into graphene/algae cells (Figure 1a), whereas no major modification was

observed when rhizobacterium was introduced into GO/algae cells (Figure 1b). However, transmittance decreased when rhizobacterium was introduced into CNT/algal cells (Figure 1c). Moreover, in the range of UV light (<300 nm), the transmittance of bio-composites was significantly reduced, which meant rhizobacterium absorbed UV light.
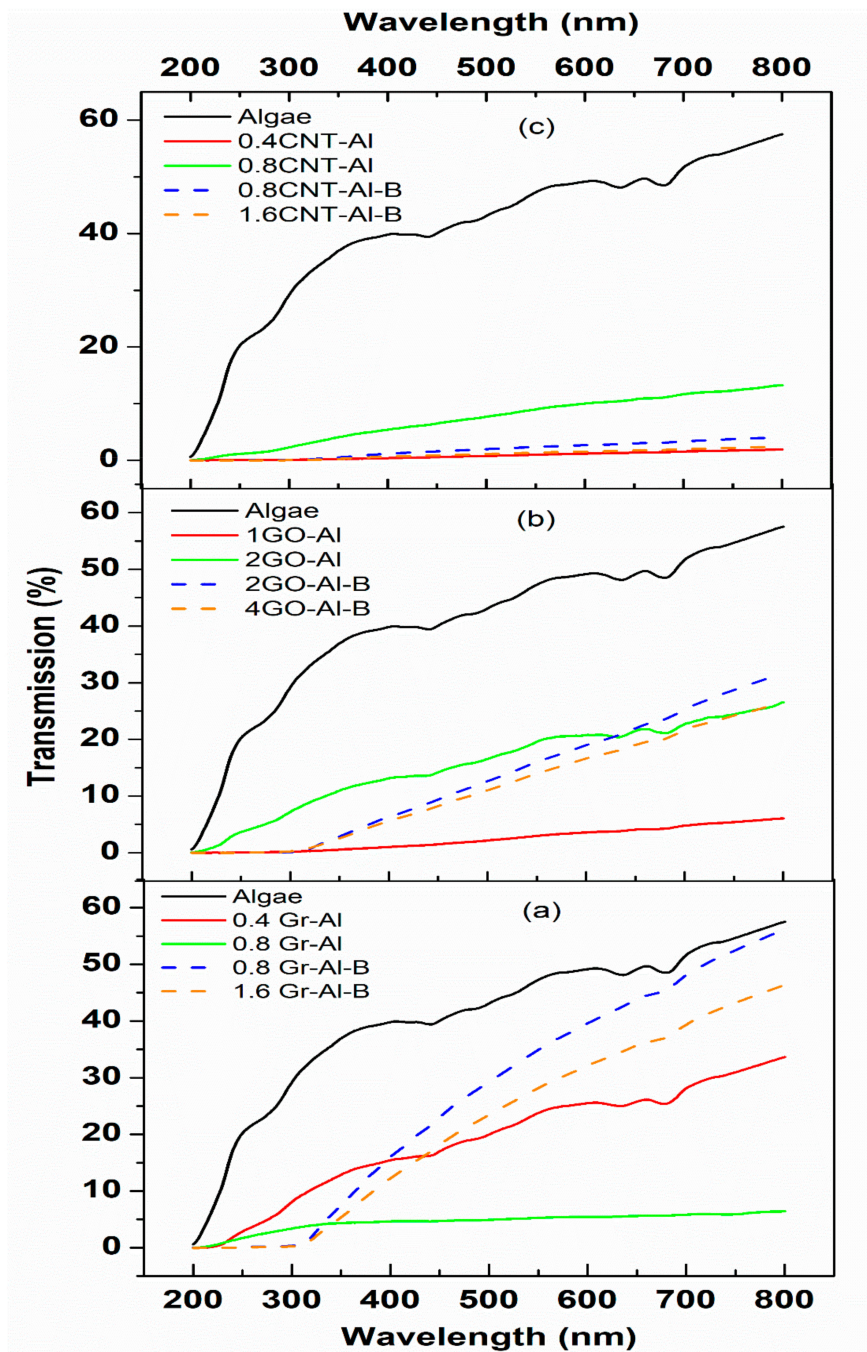

Figure 1. Transmittance characteristics of (**a**) graphene, (**b**) GO, and (**c**) CNT-based cells as compared to the reference cells (algal cells, black curve). B denotes bacterial cells and Al denotes algal cells.

Figure 2 shows the typical Raman spectrum of graphene (Gr), GO, and CNT nanomaterials obtained using a laser excitation wavelength of 633 nm in absence of biofertilsers (Figure 2a) and in presence of biofertilisers (Figure 2b). Two predominant peaks were observed at 1330 and 1595 cm^{-1} that are commonly attributed to the disorder D and crystalline G bands of carbon nanomaterials alone

with no additions, respectively [30–32]. The fluorescence was studied when an algal sample was added using a laser excitation wavelength of 785 nm. Figure 2b shows the Raman spectra of algal cells with different contents of nano-carbon materials and bacterium. For the reference algal cells (free of nano-carbon materials), the Raman spectrum showed two peaks at 1374 and 1860 cm^{-1}, respectively, which can be attributed to allenic vibration of carotenoids [33,34].
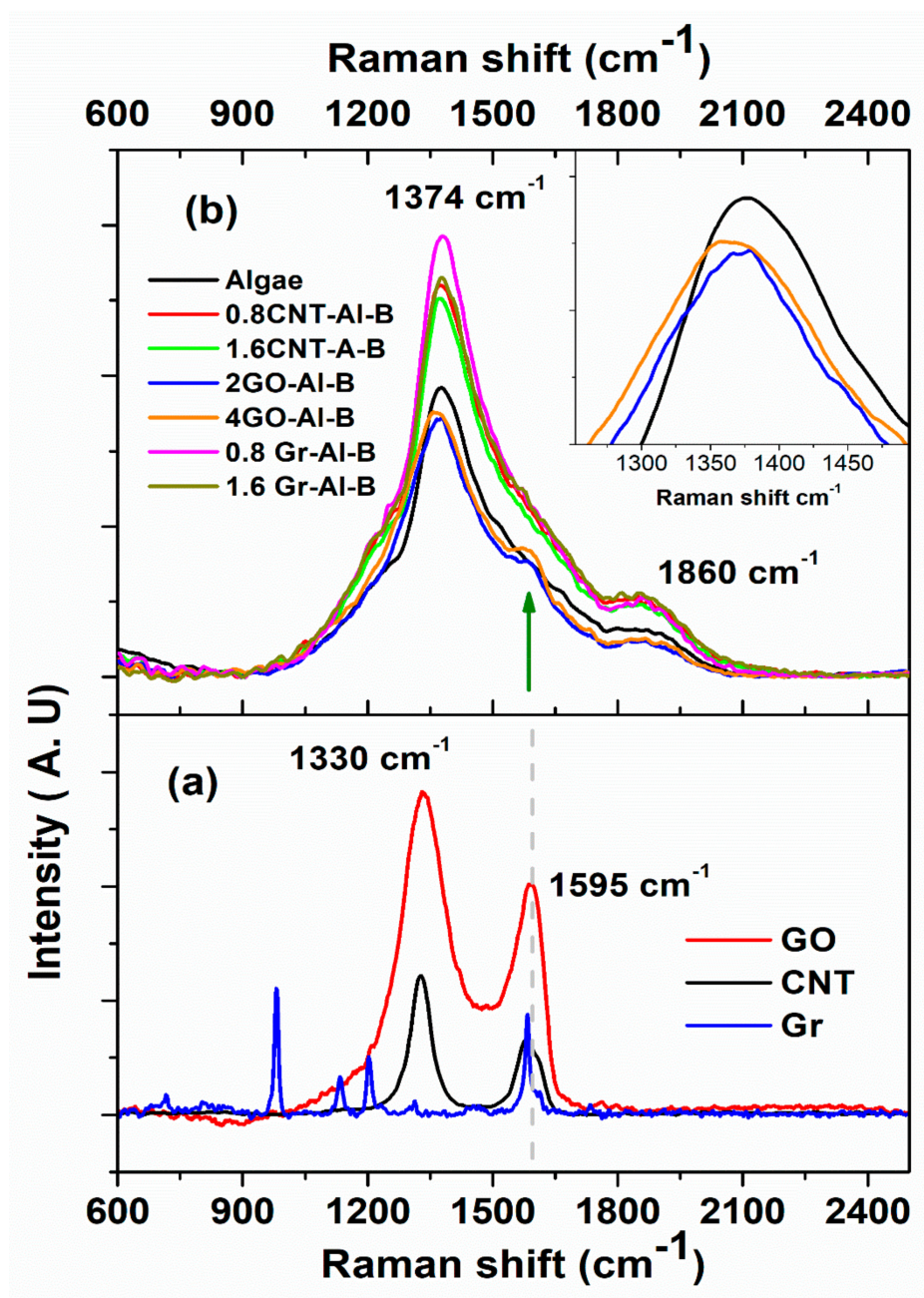
Figure 2. Raman spectra of (**a**) graphene, GO, and CNT-based cells, compared to (**b**) nano materials with the reference algal cells (Al) and bacterium (B) The green arrow indicates algal Raman shift after introducing GO.

There are two major peaks in the Figure 2b: 1374 cm^{-1}, and 1860 cm^{-1}, which are both attributed to the alga. It is noticeable that there was a shift denoted by the green arrow that indicates the interaction between algal cells and GO, as the latter is hydrophilic, which allows functionalization with biological systems. In addition, as indicated by the green arrow in Figure 2b, the Raman peak at 1374 cm^{-1} downshifted by about 13 cm^{-1} for the higher GO concentration, indicating binding or interacting

with the algal surface. Thus, this result endorses once more the hypothesis of the stability of GO in a biological medium. No major modifications were observed in the algal Raman spectra by introducing graphene or CNT.

4. Discussion

Salinity stress can have an extremely harmful effect on plant productivity. Reactive oxygen species can be produced excessively, leading to chlorophyll degradation and cell membrane oxidation as well as other destructive cellular damages [3,35]. The sodium ion is very harmful when present in the cytosol at concentrations higher than 10 mM, particularly in Germainae crops like barley. In contrast, the similarly monovalent potassium ion is maintained at a higher concentration range of 100–200 mM as it is essential for many metabolic activities in the cell [36]. Potassium acts as an activator for more than 50 enzymes, and high cytosolic Na^+ and high Na^+/K^+ ratios can be inhibitory for those enzymes [37]. Therefore, maintaining both low cytosolic Na^+ as well as a low cytosolic Na^+/K^+ ratio is essential for keeping cells functioning [38,39].

In the present study, three different salinity levels were tested, which were very close to those used by Gadwal and Naik [40]. Those levels were first tested on different plants to explore their susceptibility to salinity. As expected, salinity adversely affected the germination of the different types of seeds. However, barley was less susceptible to salinity than the broad beans. They were used in subsequent experiments that investigated the effect of the mode of application of microbial treatments, including irrigation and seed presoaking. Seed priming is a method of pre-sowing treatment that exposes seeds to certain solutions with added stimulatory components until the germination process begins [13]. The irrigation modes recorded significantly higher growth parameters, whereas the soaking in microbial treatment had the lowest parameters. This may be due to the lack of oxygen in prolonged treatments particularly for a day where complete inhibition was observed. However, the 12 h soaking treatment showed rather enhanced measurements of morphometric parameters, but they, were significantly lower than the irrigation mode. This may be attributed to the presence of living microbial cells that actively respire and consume all the oxygen.

In all modes of microbial applications tested, the germination percentage, shoot and root lengths, and fresh weight were significantly high with the combined use of cyanobacterium, rhizobacterium, and MeSA. This combined treatment resulted in the highest growth parameters. The root extension, both longitudinally and horizontally, was greatest in this treatment, and the root was noticeably stout and thick in diameter. This may be attributed to the increased transport of photosynthates to roots after application of methyl salicylate. Kalaivani et al. [13] hypothesized that MeSA may be metabolized to increase salicylic acid in the plant, which results in many changes, including increased levels of minerals and nutrient uptake through increasing root growth.

The mechanisms by which different microbial treatments can mitigate salt stress vary greatly according to the type of microorganism and the treatment used. Recently it was revealed that treatment with a halotolerant rhizobacterial strain mitigated salt stress through production of auxin that enhanced root surface area possibly via the regulation of phytohormones and gene expression where auxins increased and abscisic acid decreased [11]. Another mechanism was through enhancing polyphenols, whose antioxidant activity is attributed to hydrogen radicals dissociated from phenolic compounds [11]. The utilization of beneficial soil microbiota colonizing the rhizosphere (e.g., rhizobacteria) provides the plant with growth promoting metabolites that increase plant growth and enhance the plant's heavy metal resistance. Therefore, it has been used as a significant tool for phytoremediation and increasing plant biomass [41]. Plant growth-promoting rhizobacteria increase plant biomass by several mechanisms including; fixation of atmospheric nitrogen, mitigation of stress by using 1-aminocyclopropane-1-carboxylic acid as a unique N source, manufacture of siderophores and anti-pathogenic substances, manufacture of plant growth controllers, and the conversion of nutrient elements such as phosphorous and potassium [42]. Interestingly, similar synergistic effect is reported

for cyanobacteria which have wide range of activities and produce vast array of bioactive compounds needed for normal plant growth [43].

With regard to methyl salicylate, Kalaivani et al. [13] reported the promoting impact of MeSA seed treatment on germination and early seedling growth, where it caused enhanced germination and growth, probably due to increased salicylic acid in plant cells. Almeida et al. [44] reported that MeSA treatment greatly accelerated germination in wheat and barley seeds. According to Yusuf et al. [45], seed treatment with MeSA may help in the metabolic pentose phosphate pathway, benefiting the hydrolysis of reserves and increasing the availability of energy to the germination process and seedling emergence. This may explain the slight decrease in dry weight in our results, as the broken reserves were used for supplying energy to the germinating seedling, thereby decreasing in weight. Kalaivani et al. [13] suggested that MeSA causes an increase of SA cellular content, and according to Stout et al. [46] and Vazirimehr et al. [14], plant seeds treated with SA have higher levels of amino acids, plant growth, ion uptake, transport enzyme activity, and synthesis of plant hormones, which increase the plant responses to these proteins. These events provide significant increases in production and reduce the time for the establishment of the crop field, being more tolerant to abiotic stresses. The promoting effect of SA on shoot area may be attributed to its important roles in activation of cell division, biosynthesis of organic foods, water uptake and stomatal resistance, and better toleration of water deficit [47]. Indeed, the data of the present study support the above hypothesis, where most growth parameters increased when MeSA was supplied.

Nonetheless, the growth promoting effect of cyanobacteria is also evident from our data. Cyanobacteria have the ability to release plant growth-promoting substances, some of them are described as phytohormones like gibberellins, cytokinin, and auxin. Others are described as vitamins (vitamin B) or amino acids, toxins, and antibiotics [48]. One of the available studies investigated the effects of biofertilizer on the growth of rice (*Oryza sativa* L.). The authors reported that the presence of root-promoting hormones (auxins, cytokinin, and gibberellic acid) increased the growth of rice seedlings [49]. Žižková et al. [50] pointed out that these hormones play diverse roles in the cell, such as cell division.

Carbon nanomaterial application in ion removal and desalination is a newly trending application due to its low cost and efficient results [51]. Their negative charge as well as porosity can be useful in removing positive ions like sodium [51]. However, with the application of a combination of microbial cells with nanomaterials in one capsule, one should consider the effect of this combination on the photosynthetic activity of *Cyanothece* sp. It is interesting to note that the maximum peaks associated with chlorophyll (a) in the visible region (600–700 nm) were clearly observed for a high concentration of GO mixed with the cyanobacterium (2 GO-Al), which indicated the preservation of photosynthetic activity using this nanomaterial

The presence of shift in the spectrum when adding graphene oxide to *Cyanothece* sp. indicates the occurrence of interaction between the alga (cyanobacterium) and the graphene oxide, which is a good indication for effective co-application of the two. The application of nanomaterials with biofertilisers and MeSA mostly alleviated the inhibitory effect of salinity but with varying reponses from the two plant types. Barley responded positively to all nanomaterials tested while broad beans only responded slightly to graphene and nanocarbon tubes. This indicates that different plants can have different responses to nanomaterials and therefore future applications should test plant responses to different nanomaterials before use. Nonetheless, the alleviation of the inhibitory effect of high levels of salinity in most of the treatments emphasizes the great positive potential of the approach of combining nanomaterials, biofertilisers and methyl salicylate for mitigation of sailinity.

The smart approach illustrated in the current research lies in the use of two microorganisms with complementary and exceptional attributes. *Cyanothece* sp. is a unicellular cyanobacterium capable of alternating nitrogen fixation and photosynthesis. For nitrogen fixation to occur, a micro-aerobic environment should be available, with the heterotrophic bacteria respiring alongside the cyanobacterium itself, oxygen is consumed and CO_2 is produced during respiration, thereby allowing photosynthesis to

occur. In the absence of oxygen, nitrogen is fixed into ammonia, which is a fertilizer itself. The agar used for casing the capsule components is a commonly used solid growth medium for these microorganisms with a degree of transparency that allows light to penetrate and the cyanobacterium to perform photosynthesis. One additional exceptional attribute of *Cyanothece* sp. is its ability to transform ions found in high concentrations into elemental nanoparticles [52]. This can be very useful in a niche suffering from high ion concentrations like salinized soils. On the other frontier, nanomaterials have a high surface area that can allow ion removal from a soil–salt solution when irrigated with saline water, thereby mitigating salinity without exhibiting a toxic effect on plants or algal vitality. Indeed, [53] reported the safe use on the *Chlorella* alga when trapped in a nanomaterial layer without losing its vitality. In addition, [54] showed that graphite nanoparticle addition to fertilizers did not inhibit plant yield.

With regard to fate of biofertilisers when released from capsule, the rhizobacterium is expected to colonize the root zone and allow for a more efficient water and nutrients absorption. *Enterobacter cloacae*, specifically, was previously reported to be halotolerant and phosphate solubilizing [55]. The cyanobacterium, when released, would also allow for bioavailability of nutrients and nitrogen fixation. Nanomaterials tested mostly proved to be stimulatory to growth in most of cases under highest salinity level tested but with varying degrees and different effects on different plants. Hence, the current research opens the door for further exploitations of nanomaterials and biofertilizers in cases of salinity alleviation and mitigation.

5. Conclusions

The current research shows a smart approach of integrating biological systems with physical materials to counteract salinity. Combining the cyanobacterial strain with the rhizobacterial strain showed successful integration. *Cyanothece* sp., which is a nitrogen-fixing and photosynthetic cyanobacterium, was integrated with a heterotrophic bacterium that actively respires and consumes oxygen, thereby allowing nitrogen fixation and production of CO_2 during respiration and consequently facilitating photosynthesis. The nanomaterials have a high surface area and can act as desalinizing agents and ion removers from a soil–salt solution when irrigated with saline water, thereby mitigating salinity. Graphene oxide is the most plausible candidate because of its hydrophilicity and favorable spectral interaction with algae with no detectable inhibition of photosynthesis. The rhizobacterium, when released from a capsule or supplied in the mulch, will colonize the root zone and allow for more efficient water and nutrient absorption as it produces a growth hormone that enhances root growth. Similarly, the cyanobacterium, when released, would also allow for bioavailability of nutrients and nitrogen fixation, as well as production of an array of growth hormones and bio-stimulants. Graphene oxide and graphene represent good candidates for inclusion with biofertilizers in the treatment of salinized soils but again the type of plant should be considered. The whole combination can be used as soil mulch or in capsules. The whole capsulated combination can be readily sold to farmers to treat salinity-affected soils as supplementary fertilizer materials.

References

1. Çavuşoğlu, K.; Kabar, K. Effects of hydrogen peroxide on the germination and early seedling growth of barley under NaCl and high temperature stresses. *Eurasian J. Biosci.* **2010**, *4*, 70–79. [CrossRef]
2. Thakur, M.; Sharma, A.D. Salt Stress and Phytohormone (ABA)-Induced Changes in Germination, Sugars and Enzymes of Carbohydrate Metabolism in Sorghum bicolor (L.) Moench Seeds. *J. Agric. Soc. Sci.* **2005**, *1*, 89–93.
3. Patel, P.; Kajal, S.; Patel, V.R.; Patel, V.; Khristi, S.M. Impact of salt stress on nutrient uptake and growth of cowpea. *Bra. J. Plant Physiol.* **2010**, *22*, 43–48. [CrossRef]
4. Munns, R. Genes and salt tolerance: Bringing them together. *New Phytol.* **2005**, *167*, 645–663. [CrossRef] [PubMed]
5. Brahmaprakash, G.; Kumar Sahu, P. Reviews Biofertilizers for Sustainability. *J. Ind. Inst. Sci.* **2012**, *92*, 37–62.
6. Ahemad, M.; Kibret, M. Mechanisms and applications of plant growth promoting rhizobacteria: Current perspective. *J. King Saud Univ. Sci.* **2014**, *26*, 1–20. [CrossRef]
7. Rodríguez, A.; Stella, A.; Storni, M.; Zulpa, G.; Zaccaro, M. Effects of cyanobacterial extracellular products and gibberellic acid on salinity tolerance in Oryza sativa L. *Saline Syst.* **2006**, *2*, 7. [CrossRef]
8. Sergeeva, E.; Liaimer, A.; Bergman, B. Evidence for production of the phytohormone indole-3-acetic acid by cyanobacteria. *Planta* **2002**, *215*, 229–238. [CrossRef]
9. Stirk, W.A.; Ördög, V.; Van Staden, J.; Jäger, K. Cytokinin—And auxin—Like activity in Cyanophyta and microalgae. *J. Appl. Phycol.* **2002**, *14*, 215–221. [CrossRef]
10. Yadav, S.; Sinha, R.P.; Tyagi, M.B.; Kumar, A. Cyanobacterial Secondary Metabolites. *Int. J. Pharma Bio. Sci.* **2011**, *2*, 144–167.
11. Khan, M.A.; Asaf, S.; Khan, A.L.; Adhikari, A.; Jan, R.; Ali, S.; Imran, M.; Kim, K.M.; Lee, I.J. Halotolerant Rhizobacterial Strains Mitigate the Adverse Effects of NaCl Stress in Soybean Seedlings. *Biomed. Res. Int.* **2019**, *2019*. [CrossRef] [PubMed]
12. Abdul Malik, N.A.; Kumar, I.S.; Nadarajah, K. Elicitor and Receptor Molecules: Orchestrators of Plant Defense and Immunity. *Int. J. Mol. Sci.* **2020**, *21*, 963. [CrossRef]
13. Kalaivani, K.; Kalaiselvi, M.M.; Senthil-Nathan, S. Effect of methyl salicylate (MeSA), an elicitor on growth, physiology and pathology of resistant and susceptible rice varieties. *Sci. Rep.* **2016**, *6*, 1–11. [CrossRef]
14. Vazirimehr, M.R.; Rigi, K. Effect Of Salicylic Acid In Agriculture. *Int. J. Plant Anim. Environ. Sci.* **2014**, *4*, 291–296.
15. Wang, Y.; Voronin, G.A.; Zerda, T.W.; Winiarski, A. SiC-CNT nanocomposites: High pressure reaction synthesis and characterization. *J. Phys. Condens. Matter.* **2006**, *18*, 275–282. [CrossRef]
16. Gubicza, J.; Ungár, T.; Wang, Y.; Voronin, G.; Pantea, C.; Zerda, T.W. Microstructure of diamond-SiC nanocomposites determined by X-ray line profile analysis. *Diam. Relat. Mater.* **2006**, *15*, 1452–1456. [CrossRef]
17. Wang, Y.; Zerda, T.W. The mechanism of the solid-state reaction between carbon nanotubes and nanocrystalline silicon under high pressure and at high temperature. *J. Phys. Condens. Matter.* **2006**, *18*, 2995–3003. [CrossRef]
18. Wang, Y.; Zerda, T.W. Microstructure evaluations of carbon nanotube/diamond/silicon carbide nanostructured composites by size–strain line-broadening analysis methods. *J. Phys. Condens. Matter.* **2007**, *19*, 356205. [CrossRef]
19. Kim, K.S.; Park, S.J. Influence of multi-walled carbon nanotubes on the electrochemical performance of graphene nanocomposites for supercapacitor electrodes. *Electrochim. Acta* **2011**, *56*, 1629–1635. [CrossRef]
20. Zhu, Y.; Murali, S.; Cai, W.; Li, X.; Suk, J.W.; Potts, J.R.; Ruoff, R.S. Graphene and graphene oxide: Synthesis, properties, and applications. *Adv. Mater.* **2010**, *22*, 3906–3924. [CrossRef]
21. Lee, S.Y.; Chong, M.H.; Rhee, K.Y.; Park, S.J. Silver-coated graphene electrode produced by electrolytic deposition for electrochemical behaviors. *Curr. Appl. Phys.* **2014**, *14*, 1212–1215. [CrossRef]
22. Georgakilas, V.; Tiwari, J.N.; Kemp, K.C.; Perman, J.A.; Bourlinos, A.B.; Kim, K.S.; Zboril, R. Noncovalent Functionalization of Graphene and Graphene Oxide for Energy Materials, Biosensing, Catalytic, and Biomedical Applications. *Chem. Rev.* **2016**, *116*, 5464–5519. [CrossRef]
23. Gupta, S.; Murthy, C.N.; Prabha, C.R. Recent advances in carbon nanotube based electrochemical biosensors. *Int. J. Biol. Macromol.* **2018**, *108*, 687–703. [CrossRef] [PubMed]
24. Foo, M.E.; Gopinath, S.C.B. Feasibility of graphene in biomedical applications. *Biomed. Pharm.* **2017**, *94*, 354–361. [CrossRef] [PubMed]

25. Yang, Y.; Asiri, A.M.; Tang, Z.; Du, D.; Lin, Y. Graphene based materials for biomedical applications. *Mater. Today* **2013**, *16*, 365–373. [CrossRef]

26. El Semary, N.A.; Fouda, M. Anticancer activity of *Cyanothece* sp. strain extracts from Egypt: First record. *Asian Pac. J. Trop. Biomed.* **2015**, *5*, 992–995. [CrossRef]

27. Xin, H.; Tang, Y.; Liu, S.; Yang, X.; Xia, S.; Yin, D.; Yu, S. Impact of Graphene Oxide on Algal Organic Matter of Microcystis aeruginosa. *ACS Omega* **2018**, *3*, 16969–16975. [CrossRef]

28. Nogueira, P.F.M.; Nakabayashi, D.; Zucolotto, V. The effects of graphene oxide on green algae Raphidocelis subcapitata. *Aquat. Toxicol.* **2015**, *166*, 29–35. [CrossRef]

29. Handy, R.D.; van den Brink, N.; Chappell, M.; Mühling, M.; Behra, R.; Dušinská, M.; Simpson, P.; Ahtiainen, J.; Jha, A.N.; Seiter, J.; et al. Practical considerations for conducting ecotoxicity test methods with manufactured nanomaterials: What have we learnt so far? *Ecotoxicology* **2012**, *21*, 933–972. [CrossRef]

30. Rezgui, K.; Othmen, R.; Cavanna, A.; Ajlani, H.; Madouri, A.; Oueslati, M. The improvement of InAs/GaAs quantum dot properties capped by Graphene. *J. Raman Spectrosc.* **2013**, *44*, 1529–1533. [CrossRef]

31. Othmen, R.; Rezgui, K.; Cavanna, A.; Arezki, H.; Gunes, F.; Ajlani, H.; Madouri, A.; Oueslati, M. Improvement of the quality of graphene-capped InAs/GaAs quantum dots. *J. Appl. Phys.* **2014**, *115*, 214309. [CrossRef]

32. Shang, J.; Ma, L.; Li, J.; Ai, W.; Yu, T.; Gurzadyan, G.G. The Origin of Fluorescence from Graphene Oxide. *Sci. Rep.* **2012**, *2*, 792. [CrossRef]

33. End de Oliveira, V.; Neves Miranda, M.A.; Carolina Silva Soares, M.; Edwards, H.G.; Fernando Cappa de Oliveira, L. Study of carotenoids in cyanobacteria by Raman spectroscopy. *Spectrochim. Acta Part A Mol. Biomol. Spectrosc.* **2015**, *150*, 373–380. [CrossRef]

34. Maia, L.F.; de Oliveira, V.E.; de Oliveira, M.E.R.; Fleury, B.G.; de Oliveira, L.F.C. Polyenic pigments from the Brazilian octocoral Phyllogorgia dilatata Esper, 1806 characterized by Raman spectroscopy. *J. Raman Spectrosc.* **2012**, *43*, 161–164. [CrossRef]

35. Kang, S.M.; Khan, A.L.; Waqas, M.; You, Y.H.; Kim, J.H.; Kim, J.G.; Hamayun, M.; Lee, I.J. Plant growth-promoting rhizobacteria reduce adverse effects of salinity and osmotic stress by regulating phytohormones and antioxidants in Cucumis sativus. *J. Plant Interact.* **2014**, *9*, 673–682. [CrossRef]

36. Tester, M.; Davenport, R. Na+ tolerance and Na+ transport in higher plants. *Ann. Bot.* **2003**, *91*, 503–527. [CrossRef]

37. Munns, R.; James, R.A.; Läuchli, A. Approaches to Increasing the Salt Tolerance of Wheat and Other Cereals. In Proceedings of the Journal of Experimental Botany; Oxford Academic: Oxford, UK, 2006; Volume 57, pp. 1025–1043.

38. Kader, M.A.; Lindberg, S. Cytosolic calcium and pH signaling in plants under salinity stress. *Plant Signal. Behav.* **2010**, *5*, 233–238. [CrossRef]

39. Rubio, F.; Gassmann, W.; Schroeder, J.I. Sodium-driven potassium uptake by the plant potassium transporter HKT1 and mutations conferring salt tolerance. *Science* **1995**, *270*, 1660–1663. [CrossRef]

40. Gadwal, R.; Naik, G.R. A Comparative Study on the Effect of salt stress on seed germination and early seedling growth of two Hibiscus species. *IOSR J. Agric. Vet. Sci.* **2014**, *7*, 90–96. [CrossRef]

41. Lal, S.; Kumar, R. Exploration of heavy metal resistant rhizobacteria Enterobacter cloacae PC3 to enhance growth and metal remediation potential of Zea mays L. under Cd and Pb stress. *Int. J. Emerg. Technol. Innov. Res.* **2019**, *6*, 576–587.

42. Lal, S.; Kumar, R.; Ahmad, S.; Dixit, V.K.; Berta, G. Exploring the survival tactics and plant growth promising traits of root-associated bacterial strains under Cd and Pb stress: A modelling based approach. *Ecotoxicol. Env. Saf.* **2019**, *170*, 267–277. [CrossRef]

43. Prasanna, R.; Sood, A.; Jaiswal, P.; Nayak, S.; Gupta, V.; Chaudhary, V.; Joshi, M.; Natarajan, C. Rediscovering cyanobacteria as valuable sources of bioactive compounds (Review). *Appl. Biochem. Microbiol.* **2010**, *46*, 119–134. [CrossRef]

44. Almeida, A. Physiological Performance of Wheat and Barley Seeds Treated with Bioactivator. *Am. J. Exp. Agric.* **2012**, *2*, 90–101. [CrossRef]

45. Yusuf, M.; Hayat, S.; Alyemeni, M.N.; Fariduddin, Q.; Ahmad, A. Physiological Roles in Plants. In *Salicylic Acid*; Springer: Amsterdam, The Netherlands, 2013; pp. 15–30.

46. Stout, M.J.; Thaler, J.S.; Thomma, B.P.H.J. Plant-mediated interactions between pathogenic microorganisms and herbivorous arthropods. *Annu. Rev. Entomol.* **2006**, *51*, 663–689. [CrossRef] [PubMed]

47. Larqué-Saavedra, A.; Martin-Mex, R. Effects of salicylic acid on the bioproductivity of plants. In *Salicylic Acid: A Plant Hormone*; Springer: Amsterdam, The Netherlands, 2007; pp. 15–23.

48. Singh, R.; Parihar, P.; Singh, M.; Bajguz, A.; Kumar, J.; Singh, S.; Singh, V.P.; Prasad, S.M. Uncovering potential applications of cyanobacteria and algal metabolites in biology, agriculture and medicine: Current status and future prospects. *Front. Microbiol.* **2017**, *8*, 515. [CrossRef]

49. Ronga, D.; Biazzi, E.; Parati, K.; Carminati, D.; Carminati, E.; Tava, A. Microalgal Biostimulants and Biofertilisers in Crop Productions. *Agronomy* **2019**, *9*, 192. [CrossRef]

50. Žižková, E.; Kubeš, M.; Dobrev, P.I.; Přibyl, P.; Šimura, J.; Zahajská, L.; Drábková, L.Z.; Novák, O.; Motyka, V. Control of cytokinin and auxin homeostasis in cyanobacteria and algae. *Ann. Bot.* **2017**, *119*, 151–166. [CrossRef]

51. Hebbar, R.S.; Isloor, A.M.; Inamuddin; Asiri, A.M. Carbon nanotube—And graphene-based advanced membrane materials for desalination. *Environ. Chem. Lett.* **2017**, *15*, 643–671. [CrossRef]

52. Younis, N.S.; Bakir, E.M.; Mohamed, M.E.; El Semary, N.A. Cyanobacteria as Nanogold Factories II: Chemical Reactivity and anti-Myocardial Infraction Properties of Customized Gold Nanoparticles Biosynthesized by Cyanothece sp. *Mar. Drugs* **2019**, *17*, 402. [CrossRef] [PubMed]

53. Wahid, M.; Eroglu, E.; Chen, X.; Smith, S.; Raston, C. Entrapment of *Chlorella vulgaris* cells within graphene oxide layers. *RSC Adv.* **2013**, *3*, 8180–8183. [CrossRef]

54. Padorf, M.; Pourzahedi, L.; Gilbertson, L.; Lowry, G.V.; Herckes, P.; Westerhoff, P. Graphite nanoparticle addition to fertilizers reduces nitrate leaching in growth of lettuce (*Lactuca sativa*). *Environ. Sci.* **2020**, *7*, 127–138.

55. Hafeez, M.; Ramteke, P.; Lawrence, R.; Suresh, B.G.; Kumari, S.; Singh, A.; Singla, A.; Paul, A.; Masih, S.; Masih, H.; et al. Bio-formulation of Halotolerant Phosphate Solubilizing Enterobacter cloacae HFZ-H4 Strain to Screen Different Carrier Materials and their Shelf Life Study. *Int. J. Curr. Microbiol. Appl. Sci.* **2018**, *7*, 2373–2380. [CrossRef]